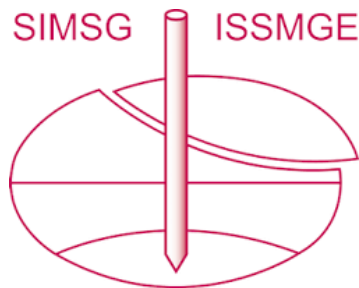


INTERNATIONAL SOCIETY FOR SOIL MECHANICS AND GEOTECHNICAL ENGINEERING



This paper was downloaded from the Online Library of the International Society for Soil Mechanics and Geotechnical Engineering (ISSMGE). The library is available here:

<https://www.issmge.org/publications/online-library>

This is an open-access database that archives thousands of papers published under the Auspices of the ISSMGE and maintained by the Innovation and Development Committee of ISSMGE.

The paper was published in the Proceedings of the 8th International Symposium on Deformation Characteristics of Geomaterials (IS-PORTO 2023) and was edited by António Viana da Fonseca and Cristiana Ferreira. The symposium was held from the 3rd to the 6th of September 2023 in Porto, Portugal.

Laboratory investigation of the cyclic loading behaviour of intact and de-structured chalk

Tingfa Liu^{1#}, Reza Ahmadi-Naghadeh², Ken Vinck³, Richard J. Jardine³, Stavroula Kontoe^{3,4},
Róisín M. Buckley⁵, Byron W. Byrne⁶, and Ross A. McAdam⁷

¹University of Bristol, Department of Civil Engineering, Bristol, United Kingdom

²Jönköping University, Department of Construction Engineering and Lighting Science, Jönköping, Sweden

³Imperial College London, Department of Civil and Environmental Engineering, London, United Kingdom

⁴University of Patras, Department of Civil Engineering, Patras, Greece

⁵University of Glasgow, School of Engineering, Glasgow, United Kingdom

⁶University of Oxford, Department of Engineering Science, Oxford, United Kingdom

⁷Ørsted Power (UK) Ltd, London, United Kingdom

Corresponding author: tingfa.liu@bristol.ac.uk

ABSTRACT

Chalk is a soft biomicrite composed of silt-sized crushable CaCO₃ aggregates. Chalk's response to cyclic loading depends critically on its sensitive micro fabric and state, which may be altered significantly by high-pressure compression, dynamic impact or prior large-strain repetitive shearing. This paper reports high-resolution undrained cyclic triaxial experiments on low- to medium-density intact chalk and chalk de-structured by dynamic compaction to model the effects of percussive pile driving. The intact chalk manifested stable and nearly linear visco-elastic response under a wide range of the one-way, stress-controlled cyclic loading conditions imposed. However, high level cycling led to sudden failures that resembled the fatigue response of metals, concretes and rocks, with little sign of cyclic damage before sharp pore pressure reductions, non-uniform displacements and finally brittle collapses. However, the de-structured chalk's response to high-level undrained cycling resembles that of silts, developing both contractive and dilative phases that led to pore pressure build-up, leftward effective stress-path drift, permanent strain accumulation, cyclic stiffness losses and increasing damping ratios. Results from exemplar tests are presented to illustrate these key features and demonstrate how chalk's undrained cyclic shearing characteristics depend also on effective stress level. The experimental outcomes provide significant scope for developing constitutive and empirical relationships or predictive tools to enable the interpretation and design of driven pile foundations in chalk and other chalk-structure interaction related problems under cyclic loading.

Keywords: chalk; cyclic loading; triaxial; laboratory testing.

1. Introduction

Laboratory cyclic element testing that reproduces in-situ soil states and applies representative stress conditions plays a key role in supporting the cyclic foundation design (Andersen 2009) and in particular that of open-ended driven steel piles (Jardine et al. 2012). This paper concerns the cyclic response of Chalk, a variable and very weak limestone, which is found under large areas of North-West Europe and other regions worldwide (Mortimore 2012) and is encountered at foundation depths of many onshore and offshore projects (Jardine et al. 2018, Buckley et al. 2020). Offshore structures typically experience operational cyclic loads from wind and waves, as well as occasionally extreme high-level cycling in storm or earthquake events. Representative characterisation of chalk's monotonic and cyclic behaviour is therefore critical to their safe design.

While chalks with unconfined compressive strengths (UCS) of several MPa can stand in moderately high coastal cliffs, McAdam et al. (2022) and Pedone et al. (2023) show that driven piles subjected to lateral loading can withstand relatively modest loads. Their monotonic

response is predominantly controlled by the brittle and fractured nature of the surrounding chalk mass, while their response to repetitive loading is governed by the cyclic response of the fractured 'intact' chalk.

However, the axial response of piles driven in chalk is dominated by the properties of the de-structured chalk that forms around the piles' shafts during installation. Lord et al. (2002) noted that the dynamic percussion applied during impact pile driving creates de-structured, chalk 'putty' beneath the piles' advancing tips which spreads and further softens around their shafts leading to average resistances below 20 kPa in low to medium density chalk. Buckley et al. (2018) and Vinck (2021) identified how de-structuration varies with radial distance from the axes of open steel piles considering conditions immediately after driving and after long-term ageing (at shallow depth above the water table) when the material reconsolidated over time to achieve notably lower water contents and significantly greater shear strengths. Jardine et al. (2023) show that the response of the reconsolidated putty to monotonic and cyclic loading, as well as interface shearing, is central to addressing axial capacity and cyclic loading performance for piles driven in chalk.

This paper summarises key findings from undrained cyclic triaxial studies on both intact and fully de-structured low-to-medium density chalk by Ahmadi-Naghadeh et al. (2022) and Liu et al. (2022a). The laboratory research was conducted under the ALPACA Joint Industry Project (JIP) which investigated how 37 tubular steel piles behaved under axial and lateral, monotonic and cyclic loading at the St Nicholas-at-Wade (SNW) (Kent, UK) research site (Jardine et al. 2023). The laboratory experiments on intact chalk applied stress-controlled, mainly low-strain, one-way cyclic loading, starting from both ‘in-situ’ and ‘elevated’ initial mean effective stress levels, while the parallel programme on dynamically de-structured and reconsolidated chalk spanned the two-way high-level cycling regimes that are critical for axial cyclic design of driven piles. Parallel monotonic loading experiments reported by Vinck et al. (2021, 2023) and Liu et al. (2023a) investigated intact chalk’s mechanical behaviour, as well as its anisotropic and yielding characteristics from relatively low in-situ stresses up to elevated stresses with $p_0' = 12.8$ MPa. Liu et al. (2023b) demonstrate how the cyclic experiments can be further interpreted, offering interaction diagrams and empirical correlations as well as an effective stress-based cyclic design method.

2. Sample preparation and index properties

Buckley et al. (2018), Vinck (2021) and Vinck et al. (2022) describe the profiles of the Margate and Seaford white chalk formations at SNW. All weathered material has been removed at SNW, exposing CIRIA grade B2 (Lord et al. 2002) structured, very weak to weak, low-to-medium density white structured chalk, which has mainly vertically oriented micro-fissures with 10 to 25 mm spaces that cannot be identified easily by eye.

The intact cyclic study focussed on samples prepared from $350 \times 350 \times 250$ mm chalk blocks taken at ≈ 1.4 m depth, close to the test piles. The blocks were carefully hand-trimmed in the field. All visibly fractured material was avoided. Blocks were carefully sealed on site using several layers of cling film, wax and aluminium foil before being secured in wooden boxes whose void spaces were injected with polyurethane foam. High-quality specimens were cored for testing with a high-stability radial arm drill employing water-flushing (Vinck 2021).

Uniform batches of de-structured samples were prepared through laboratory dynamic compaction in an analogous way to pile driving. An automatic ‘Proctor’ compactor applied blows at ≈ 2 s intervals with a 4.5 kg ram and a 300 mm drop height to 350–450 g chalk lumps contained in 100 mm diameter annular split mould. Manual mixing was undertaken every 50 blows to ensure uniformity and 100–150 blows were required to form ≈ 0.3 litre batches of chalk putty. The resulting mainly silt-sized putty gave 9 ± 3 kPa fall-cone undrained shear strengths. Typical index properties of the intact and de-structured chalk samples are listed in Table 1.

Table 1. Typical index properties of the SNW chalk samples

w_L (%)	I_p (%)	G_s	D_{50} (μm)	ρ_{bulk} (Mg/m^3)	w_c (%)
30.6	6.4	2.71	3.0	$1.92^\dagger / 2.0^*$	$30^\dagger / 26^*$

* Intact specimens; † de-structured specimens pre-consolidated under 70 kPa mean effective stress

3. Test equipment, procedures and programmes

Cyclic triaxial tests were performed with automated Bishop-Wesley type hydraulic stress-path apparatuses that tested approximately 38 mm diameter, 76 mm high, specimens. Diametrically opposed pairs of vertically mounted LVDT transducers (with optimal precision around 0.1 μm) were installed over the central 50 mm lengths to measure local axial strains, while external sensors measured global straining. Pore pressures were measured at the specimen bases and the tests were conducted sufficiently slowly for full pore pressure equalisation during undrained monotonic and cyclic loading. Liu et al. (2022b) detailed the equipment’s stress and strain measurements’ resolutions and precisions. A suction cap and half-ball connection system centralised the loading of the top platen. Double layers of latex membrane smeared with high vacuum grease were deployed at specimens’ tops and bases to minimize stress non-uniformity.

An ‘in-mould’ isotropic consolidation stage was implemented to form de-structured chalk samples of sufficient strength by maintaining a triaxial cell-to-back pressure difference of 70 kPa for 15 hours under drained conditions. This stage improved the soft specimens’ ability to maintain regular shapes and resist disturbance.

Typical test stages applied are illustrated in Fig. 1. The specimens were saturated by applying 300–400 kPa back pressure until $B > 0.97$, followed by isotropic consolidation at 1 kPa/minute to reach the targeted mean effective stresses (p_0'). Maintained stress creep was applied to allow the axial strain rate to diminish below 0.005%/day, which took at least 48 hours for the intact specimens and 8–12 days for the de-structured specimens. Undrained cycling was applied by holding constant cell pressures while varying deviatoric stress sinusoidally about a fixed q_{mean} by the amplitudes q_{cyc} . Relatively long periods of 300 s were adopted to enable full control, pore-pressure equalisation and detailed logging of all parameters. The intact programme was limited to compressive loading paths, imposing only one-way cycling with $q_{\text{cyc}} \leq q_{\text{mean}}$ as extension failure could only be achieved by applying cell pressures up to 4 MPa that exceed the equipment’s rated capacity. However, no such restriction applied in testing the de-structured specimens and their cycling programme was extended to cover the full two-way regime. Post-cyclic monotonic shearing to failure was applied to specimens that sustained long-term cycling without failing. Table 2 summarises the applied p_0' levels, mean and cyclic stresses, and their ratios defined in relation to average undrained shear strengths established in ‘control’ sets of monotonic shearing tests. Further details are provided by Ahmadi-Naghadeh et al. (2022) and Liu et al. (2022a).

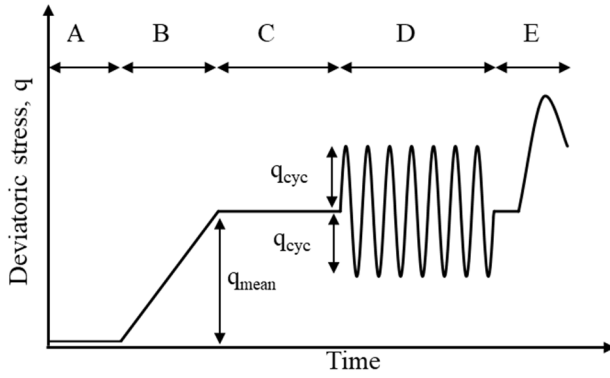


Figure 1. Schematic diagram of testing stages: A - isotropic saturation and consolidation; B - pre-shearing; C - creep; D - cyclic loading; E - post-cyclic monotonic shearing on unfailed samples; Stages B to E all undrained

Table 2. Cyclic testing programme overview

Material*	p_0' (kPa)	S_u (kPa) †	q_{mean} (kPa) ($q_{mean}/(2S_u)$)	q_{cyc} (kPa) ($q_{cyc}/(2S_u)$)
I	42	1200	750~1575 (0.31~0.66)	250~1087 (0.10~0.45)
	342	1300	975~1220 (0.38~0.47)	975~1220 (0.38~0.47)
D	200	50	-15~79 (-0.15~0.79)	17~75 (0.17~0.75)
	400	100	0 (0)	60~150 (0.30~0.75)

* I - Intact chalk, D - De-structured chalk; † Identified at the peak strengths for intact chalk and phase transformation points (PPT) for de-structured chalk.

4. Intact chalk: undrained monotonic and cyclic loading behaviour

4.1. Monotonic shearing response

Chalk specimens invariably show natural variations. Ahmadi-Naghadeh et al. (2022) noted $\pm 12\%$ deviations in shear strengths relative to means from multiple tests on sub-sampled ‘identical’ specimens, reflecting variations in micro-fissures and other imperfections. Greater variations are often found between nominally identical samples of natural cemented carbonate rocks (Acharya 2004). Fig. 2 presents typical effective stress paths from monotonic compression tests on intact specimens consolidated to in-situ $p_0' = 42$ kPa and in-situ + 300 kPa. The paths of the lower pressure tests passed close to the 3:1 gradient no tension line limit implicit in triaxial testing, before eventually failing. Modest pore pressure changes of ≈ 30 kPa developed up to peak conditions and strong reductions followed post-peak as the samples cracked and fractures tried to open. The elevated pressure tests showed, on average, higher peak q values. They also followed more steeply inclined effective stress paths, developing greater (on average 175 kPa) positive pressures up to peak, and less dilatant post-peak, pore pressure changes. These features are interpreted by Vinck et al. (2022) as reflecting the closure of minor fissures and micro-cracks during consolidation.

Fig. 2 also plots the best fit failure parameters from 41 drained and undrained monotonic triaxial tests

conducted at in-situ and in-situ + 300 kPa mean effective stress levels, giving peak Mohr-Coulomb envelope $c' = 490$ kPa and $\phi_{peak}' = 39.6^\circ$. The failures were markedly brittle, reflecting sudden losses in bond strength (or true cohesion) and the formation, or mobilisation, of discontinuities, leading to post failure states that deviated from critical states. The latter were only reached with increasing confining pressures under which intact chalk became progressively more ductile and converged towards critical states with $M = 1.25$ (equivalent to $\phi_{cs}' \approx 31^\circ$) (Liu et al. 2023a).

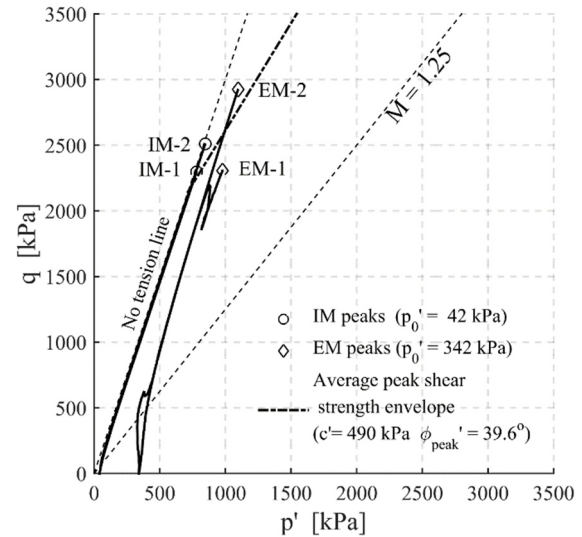


Figure 2. Pre-yeilding undrained effective stress paths and peaks for the monotonic CIU triaxial tests under in-situ ($p_0' = 42$ kPa) and elevated ($p_0' = 342$ kPa) stresses

4.2. Unstable and stable cycling behaviour

The impact of high-level, unstable, one way cycling on Intact chalk is demonstrated for an exemplar test (with $q_{mean} = 1225$ kPa, $q_{cyc} = 950$ kPa) in Figs. 3-4, showing the evolution of axial strain and pore pressure against the number of cycles, as well as the effective stress path followed. The strains and pore pressures showed little or no sign of impending instability, until $N \approx 150$. Relatively modest changes of around 0.1% axial strain and -6 kPa pore water pressure developed over the following 30 cycles before brittle failure occurred abruptly after $N_f = 181$ regular cycles, followed by significant straining and continuing decrease in pore water pressure as the specimen collapsed. The effective stress path showed no leftward drift, as is usual in tests on saturated soils, but instead, the paths remained within a tight band close to the non-tension limit until cyclic loading degraded the cemented chalk’s internal structure sufficiently for abrupt failure to occur under the imposed mean and cyclic deviatoric stresses. Fig. 5 plots the corresponding changes in the secant undrained cyclic Young’s modulus and damping ratio, which were defined from the span in strains and stresses between the peaks and troughs of each cycle. Little change was seen in either the damping ratio (which remained at around 4%) or the cyclic stiffness, which remained relatively high at around 2.9 GPa, until degradation set in over the last 30 cycles.

Minimal changes in axial strain and pore pressures were observed in lower-level cycling experiments that led to stable outcomes. The typical stable test considered in Fig. 6, which subjected its specimen to $q_{\text{mean}} = 750$ kPa, $q_{\text{cyc}} = 730$ kPa, leading to $q_{\text{max}}/(2S_u) = 0.62$ strained by just 0.05% over 16 days of cycling. Its overall strain rate was lower than the $<0.005\%$ /day residual creep rate tolerated before the start of cycling, and its pore pressure drift less than 1 kPa. As shown in Fig. 6, this specimen's behaviour could be considered as nearly linear visco-elastic, with an initial (vertical, undrained) cyclic Young's modulus around 3.5 GPa initially, that gradually rose to ≈ 3.8 GPa as cycling progressed. The specimen's damping ratio fluctuated from around 6.4% initially, to exceed 10% as N increased.

The impact of effective stress level on intact chalk's monotonic and cyclic response was investigated through two parallel tests on specimens consolidated to 300 kPa higher than the in-situ stress of $p_0' = 42$ kPa. These specimens were found to exhibit higher initial stiffness and larger positive excess pore water pressures during monotonic shearing. Fig. 7 compares the pore pressure trends for ECy-F1 and ICy-D4, which were cycled under comparable normalised ratios of $q_{\text{mean}}/(2S_u) = q_{\text{cyc}}/(2S_u) = 0.46 \pm 0.01$, but from different initial mean effective stress conditions. Also denoted are the numbers of cycles to failure (N_f) and the corresponding cyclic pore pressure amplitudes (u_r^{amp}) and pore pressure (Δu) increments up to failure. The cyclic experiments all showed modest permanent strain development up to the onset of brittle failure. However, the pore pressure of the higher p_0' ECy-F1 specimen oscillated with larger amplitudes and overall pore pressure rise of 55 kPa that led to leftwards effective stress paths drifting prior to failure. Noting their less dilatant failures, the higher p_0' tests manifested marginally more 'soil-like' responses than when cycled from 'in-situ' stresses.

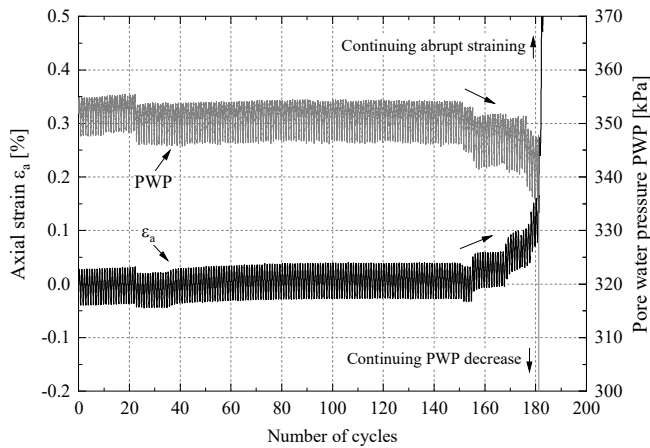


Figure 3. Typical unstable cycling response: variation of axial strain and pore water pressure against number of cycles up to failure at $N_f = 181$ ($q_{\text{mean}} = 1225$ kPa, $q_{\text{cyc}} = 950$ kPa and $q_{\text{max}}/(2S_u) = 0.91$)

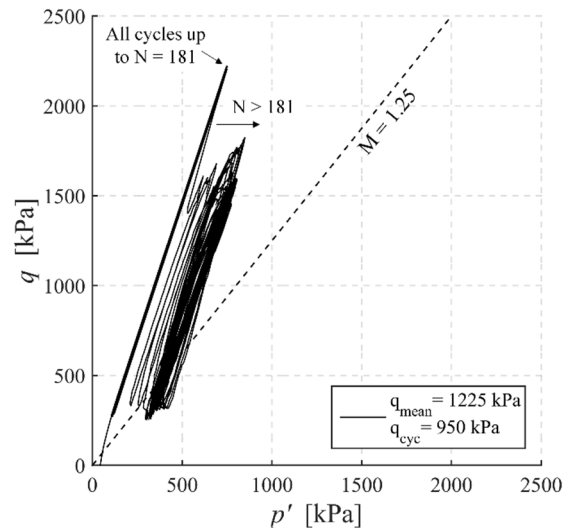


Figure 4. Effective stress path in a typical unstable cyclic test

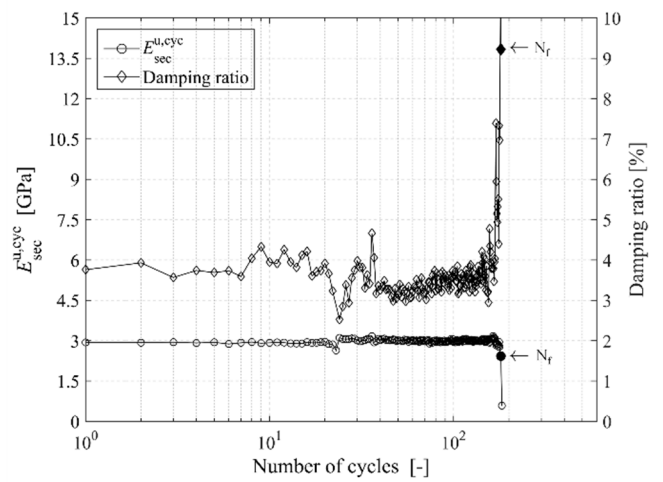


Figure 5. Unstable cycling response: evolution of cyclic stiffness and damping ratio ($q_{\text{mean}} = 1225$ kPa, $q_{\text{cyc}} = 950$ kPa)

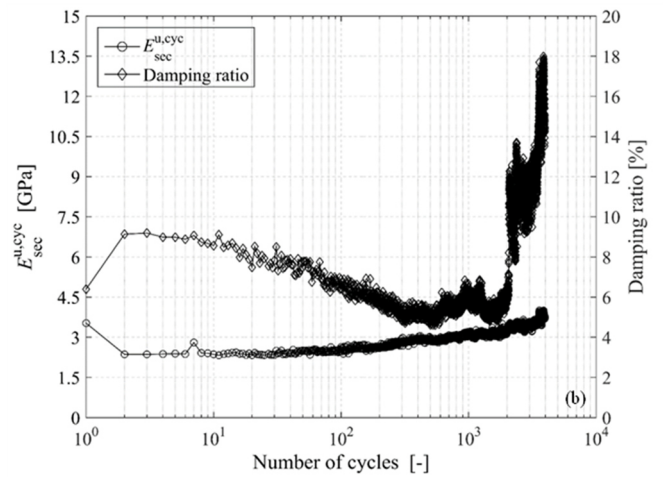


Figure 6. Evolution of cyclic stiffness and damping ratio in a typical stable cyclic test applying $q_{\text{mean}} = 750$ kPa, $q_{\text{cyc}} = 730$ kPa and $q_{\text{max}}/(2S_u) = 0.62$

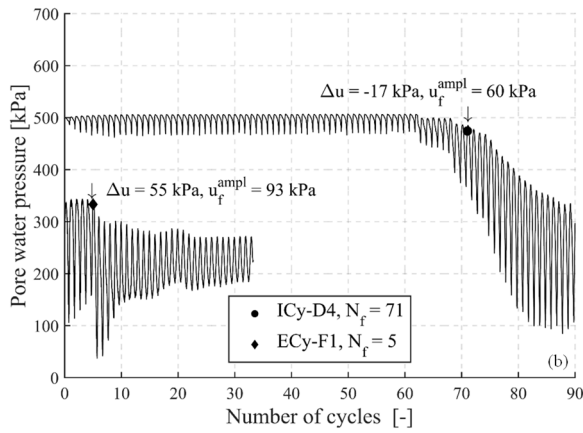


Figure 7. Pore water pressure trends for tests ICy-D4 ($p_0' = 42$ kPa) and ECy-F1 ($p_0' = 342$ kPa) with $q_{\text{mean}}/(2S_u) = q_{\text{cyc}}/(2S_u) = 0.46 \pm 0.01$

4.3. Cyclic strain accumulation and stiffness

The experimental outcomes reveal intact chalk's distinct features of strain accumulation and stiffness evolution. Figs. 8-9 demonstrate cyclic permanent strain trends for a stable group of tests subjected to low-level cycling ($q_{\text{max}}/(2S_u) \leq 0.76$) and for an unstable group under high-level cycling ($q_{\text{max}}/(2S_u) \geq 0.87$), respectively. The stable specimens exhibited 'visco-elastic' behaviour and developed minimal straining at an overall axial strain rate lower than the limit of 0.005% per day applying at the end of the creep stages. The specimens subjected to high cyclic loading levels failed after fewer cycles and gave ϵ_a/N_f ratios several orders of magnitude higher than those in the stable group. Abrupt straining was observed as failure developed and the accumulated cyclic strains did not present any systematic relationship with either N or the cyclic loading parameters.

Overall, the abrupt undrained failures of the unstable chalk tests are unlike those observed with saturated soils in which cyclic collapse is usually preceded by pore pressure rises, permanent strain accumulation, loss of cyclic stiffness and growing damping ratios (Anderson 2009). The intact chalk's behaviour appears closer to that of granites or marbles, and solids such as metals, glass or concrete - where load cycling above certain threshold levels initiates micro-shearing or cracking around inherent micro-features that generate stress concentrations. The latter initiators include micro-voids, discontinuities, sharp edges or imperfections in specimen geometry. In rocks, repeated loading prompts progressive wear and shearing between grains, forming microcracks that propagate within the matrix before coalescing into macrocracks (Cerfontaine and Collin 2018). Each load cycle within the unstable region leads to flaws growing at rates that depend on the cyclic amplitudes, mean loads and frequency, as well as confining pressures and any prior overloading in such media.

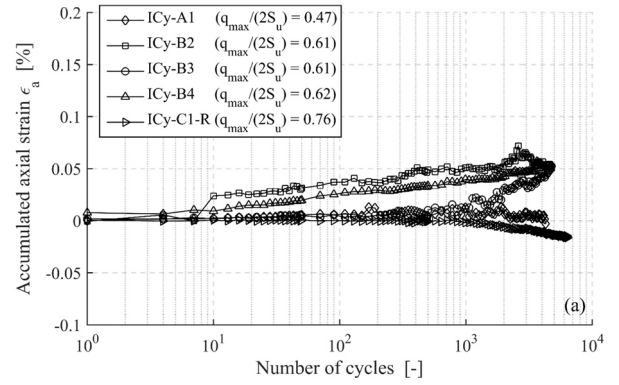


Figure 8. Development of permanent cyclic strains in the stable tests subjected to low-level cycling

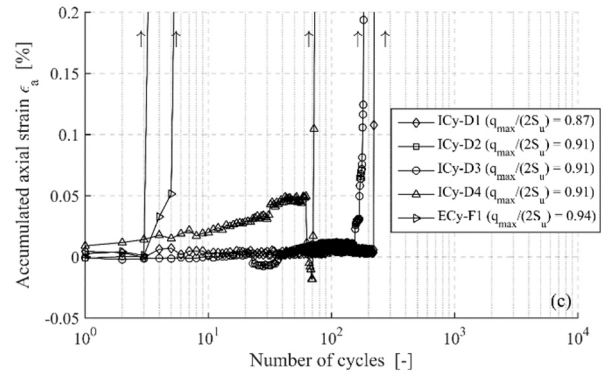


Figure 9. Cyclic permanent strains in the unstable tests under high-level cycling

5. De-structured chalk: undrained cyclic loading behaviour

5.1. Undrained monotonic loading behaviour

The dynamically compacted and re-consolidated chalk putty showed distinctly different monotonic and cyclic behaviour to its 'parent' intact chalk. As shown below, its responses to undrained shearing and cycling were far closer to those of saturated silts and silty sands.

Fig. 10 demonstrates chalk putty's response to undrained monotonic triaxial compression (TXC) and extension (TXE) with zoomed-in q - p' effective stress paths. The paths rose nearly vertically upon compression and extension shearing and rotated to follow leftward (contractive) stages after mobilising modest 'peak' resistances (after relatively small strains $\epsilon_a < 0.2\%$). Strain softening followed as shearing continued up to phase transformation (PT) points at which their paths abruptly rotated clockwise and climbed towards ultimate (critical state) conditions. Continued straining led to markedly higher ultimate strengths as the specimens attempted to dilate. The deviatoric stresses at phase transformation (PT) points were taken as indicating putty's operational monotonic shear strengths ($2S_u$), implying S_u values around 50 kPa and 100 kPa for the $p_0' = 200$ and 400 kPa tests respectively, with $S_u/p_0' = 0.25$. Specimens undergoing extension developed similarly contractive pre-PT responses to shearing, followed by dilation after reaching phase transformation, giving broadly similar, yet not fully symmetric stress paths and shear strengths to the compression tests.

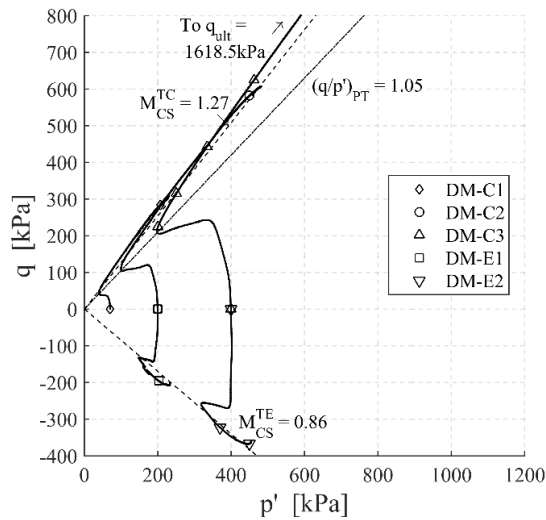


Figure 10. Effective stress paths of de-structured chalk under triaxial compression and extension

5.2. Undrained cyclic loading behaviour

Two exemplar tests, DCy-C3 ($q_{\text{mean}}/(2S_u) = 0$, $q_{\text{cyc}}/(2S_u) = 0.6$) and DCy-D4 ($q_{\text{mean}}/(2S_u) = 0.28$, $q_{\text{cyc}}/(2S_u) = 0.6$) are chosen to demonstrate de-structured chalk's typical unstable response to high-level cyclic loading. Figs 11-12 plot their stress-strain response and overall effective stress paths. Axial strain accumulation accelerated markedly as cyclic failure developed and the stress-strain curves fell initially in tight bands but fanned out as failure approached. Effective stress paths drifted leftward invariably as pore water pressures grew. The paths traversed the phase transformation points and slopes defined by monotonic loading, as well as the critical state slopes. Fig. 13 shows how the secant undrained cyclic Young's modulus and damping ratio evolved in test DCy-D4, showing systematic variation in the damping ratio and cyclic stiffness trends. Damping ratios showed maxima near failure, followed by marked post-failure reductions as cyclic strains increase.

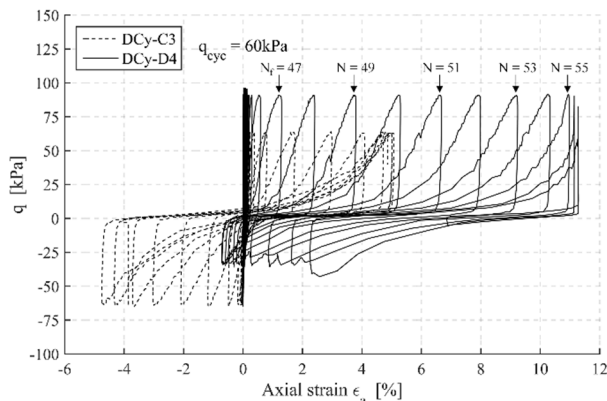


Figure 11. Stress-strain behaviour observed in unstable cyclic tests DCy-C3 and -D4

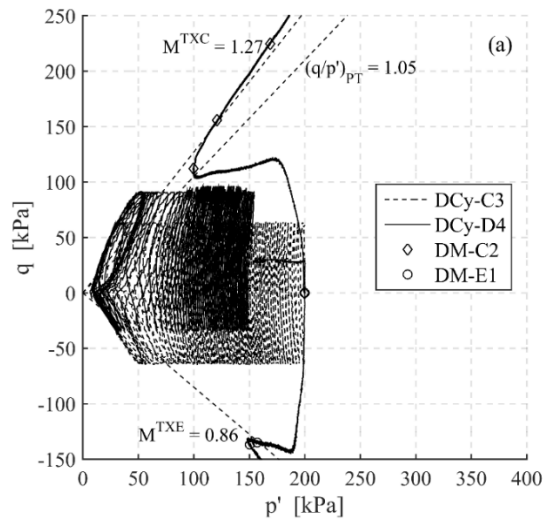


Figure 12. Stress paths development in typical unstable tests

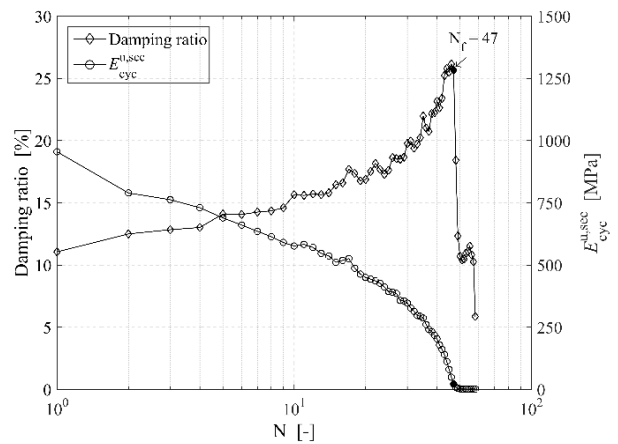


Figure 13. Damping ratio and cyclic stiffness evolution in a typical unstable test with $q_{\text{mean}}/(2S_u) = 0.28$ and $q_{\text{cyc}}/(2S_u) = 0.60$

Fig. 14 shows damping ratio and cyclic stiffness trends for a typical stable test being pre-sheared to the highest q_{mean} ($q_{\text{mean}}/(2S_u) = 0.79$) and cycled with the lowest q_{cyc} ($q_{\text{cyc}}/(2S_u) = 0.17$). The specimen sustained > 10,000 cycles and accumulated only small axial strains. The stress-strain loops evolved steadily, showing moderately increasing cyclic stiffness and decreasing damping ratio. Applying large number of such low-level cycles resulted in a stable, non-linear, but principally reversible response that enhanced the de-structured chalk's cyclic resistances. Liu et al. (2022a) provided further details on how the accumulated cyclic strain may be expressed with power-law equations with parameters that were correlated with the mean and cyclic stress ratios.

As noted in Table 2, parallel tests were performed on de-structured specimens consolidated to higher pressures with $p_0' = 400$ kPa (with $q_{\text{mean}} = 0$). These specimens exhibited broadly compatible cyclic patterns to the $p_0' = 200$ kPa experiments, although the higher-pressure tests developed lower (absolute) strains at failure and higher cyclic stiffness values under similar normalised loading levels. However, higher excess pore water pressure ratios were observed in the higher p_0' tests, suggesting higher susceptibility to lower amplitude cyclic loading. Fig. 15 gives further details on how the stress path loops evolved

in Tests DCy-B1 ($p_0' = 200$ kPa) and DCy-B1-E ($p_0' = 400$ kPa), both with $q_{\text{mean}}/(2S_u) = 0$ and $q_{\text{cyc}}/(2S_u) = 0.45$. Cyclic phase transformation points can be identified from the effective stress path loops, indicating $(q/p')_{\text{PT}}^{\text{cyc}}$ gradients of ≈ 0.54 and 0.38 in compression and extension respectively. The corresponding shear resistance angle was largely independent of p_0' level and loading directions.

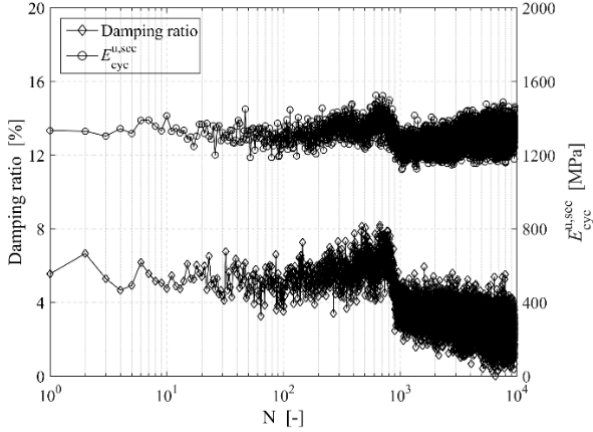


Figure 14. Damping ratio and cyclic stiffness evolution in a typical stable test with $q_{\text{mean}}/(2S_u) = 0.79$ and $q_{\text{cyc}}/(2S_u) = 0.17$

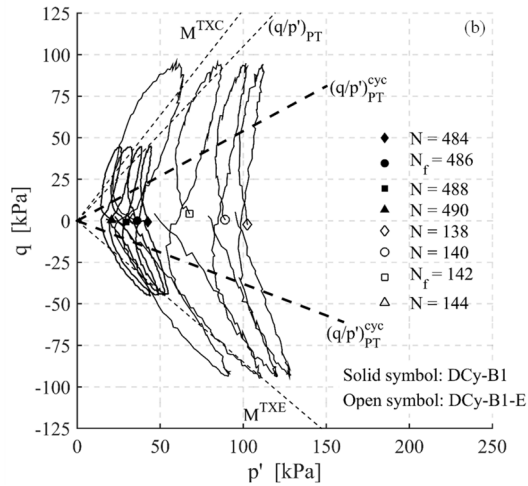


Figure 15. Selected stress path loops near cyclic failure for Tests DCy-B1 ($p_0' = 200$ kPa) and -B1-E ($p_0' = 400$ kPa), both applying $q_{\text{mean}}/(2S_u) = 0$ and $q_{\text{cyc}}/(2S_u) = 0.45$

5.3. Comparison of intact and puttified chalk

Dynamic percussion applied by laboratory compaction or in-situ pile installation degrades intact chalk to form soft putty with shear strength ≈ 100 times lower than that of the brittle ‘parent’ material. Direct comparison between their undrained cyclic triaxial behaviours is demonstrated in Fig. 16, drawing on representative paired tests that applied identical mean and cyclic stress ratios of $q_{\text{cyc}}/(2S_u) = q_{\text{mean}}/(2S_u) \approx 0.44$. Cyclic failure is preceded in the putty by pore pressure build-up, leftward drifting of the effective stress paths, growing cyclic stiffness losses and damping ratios. In contrast, the intact chalk shows a very stiff cyclic response, with little or no sign of impending instability, until shortly before abrupt brittle failure. As shown in Fig. 16(b), the intact chalk’s cyclic effective stress paths remained within a tight band prior to failure and drifted

rightward, with markedly dilative pore pressures developing as the chalk’s internal structure collapsed. As concluded above, intact chalk’s cyclic behaviour is closely analogous to that of harder rocks and solid materials such as metals, whose cyclic or fatigue failure is dominated by their inherent micro-structures and whose failure is triggered by local stress concentrations that promote progressive wear and shearing.

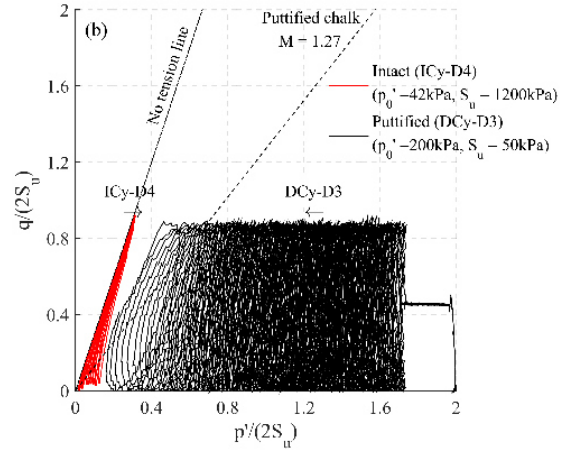
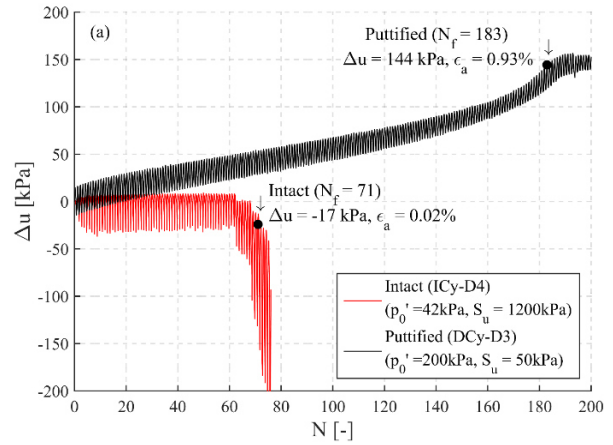


Figure 16. Undrained cyclic behaviour of intact and puttified chalk ($q_{\text{cyc}}/(2S_u) = q_{\text{mean}}/(2S_u) \approx 0.44$): (a) excess pore water pressure variation; (b) effective stress path in normalised $q/(2S_u)-p'/(2S_u)$ space (plotted up to $N_f + 3$ cycle)

6. Conclusions

Only limited information exists on how cyclic loading affects the behaviour of natural intact and de-structured chalk. However, understanding their cyclic loading behaviour is crucial to a range of chalk-structure interaction problems, including the design of open steel driven piles for offshore and onshore structures. This paper summarises the key element testing outcomes from comprehensive laboratory cyclic triaxial studies on intact and fully de-structured low- to medium-density chalk that led to new cyclic pile design approaches under the ALPACA project. The key conclusions drawn are:

- (1) Intact chalk provides little indication of cyclic damage developing until shortly before failure, especially in tests conducted from in-situ stresses. Collapse appears to involve changes in the chalk’s internal structure that only become apparent as failure approaches.

- (2) Intact chalk manifests a nearly visco-elastic behaviour applies over a relatively extensive range of stable cyclic conditions, within which stiffness improves over thousands of cycles, without any loss of undrained shear strength.
- (3) Intact chalk's response varies with pressure level, with more positive cyclic pore pressure changes and significantly less dilative trends developing after consolidation to elevated pressures
- (4) The response of re-consolidated de-structured chalk to undrained monotonic and cyclic loading differs markedly from that of intact chalk, resembling that of silts and silty-sands, developing well-defined phase transformation (PT) and critical states over medium-to-large strains.
- (5) Reconsolidated putty's response to undrained high-level cyclic loading involves an overall trend for positive pore pressure build-up, leftward effective stress path drift, permanent strain accumulation, gradual cyclic stiffness losses and increasing damping ratios.
- (6) De-structured specimens consolidated to different pressure levels manifest broadly similar overall cyclic loading responses, although raising the pressures increases the reconsolidated putty's susceptibility to lower amplitude cyclic loading.

Acknowledgements

The experimental studies were undertaken under the ALPACA project funded by the Engineering and Physical Science Research Council (EPSRC) grant EP/P033091/1, Royal Society Newton Advanced Fellowship NA160438 and Supergen ORE Hub 2018 (EPSRC EP/S000747/1). Byrne is supported by the Royal Academy of Engineering under the Research Chairs and Senior Research Fellowships scheme. The authors acknowledge additional financial and technical support by Atkins, Cathie Associates, Equinor, Fugro, Geotechnical Consulting Group (GCG), Iberdrola, Innogy, LEMS, Ørsted, Parkwind, Siemens, TATA Steel and Vattenfall. Imperial College's EPSRC Centre for Doctoral Training (CDT) in Sustainable Civil Engineering and the DEME Group (Belgium) supported Ken Vinck. Socotec UK Ltd and Fugro carried out the block sampling and rotary core sampling campaigns. Invaluable technical support by Steve Ackerley, Graham Keefe, Prash Hirani, Stef Karapanagiotidis, Graham Nash and Gary Jones at Imperial College London is acknowledged gratefully.

References

- Acharya, S. S. 2004 "Characterisation of cyclic behaviour of calcite cemented soils". PhD Thesis, University of Western Australia.
- Ahmadi-Naghadeh, R., T. Liu, K. Vinck, R. J. Jardine, S. Kontoe, B. W. Byrne, R. A. McAdam. 2022 "Laboratory characterisation of the response of intact chalk to cyclic loading". Ahead of Print in *Géotechnique*. <https://doi.org/10.1680/jgeot.21.00198>
- Andersen, K. 2009. "Bearing capacity under cyclic loading - Offshore, along the coast, and on land". *Canadian Geotechnical Journal*, 46 (5), 513–535. <https://doi.org/10.1139/T09-003>
- Buckley, R. M., R. J. Jardine, S. Kontoe, D. Parker, F. C. Schroeder 2018. "Ageing and cyclic behaviour of axially loaded piles driven in chalk". *Géotechnique*, 68(2):146-161. <https://doi.org/10.1680/jgeot.17.P.012>
- Buckley, R. M., R. J. Jardine, S. Kontoe, P. Barbosa, F. C. Schroeder 2020. "Full-scale observations of dynamic and static axial responses of offshore piles driven in chalk and tills". *Géotechnique*, 70(8): 657-681. <https://doi.org/10.1680/jgeot.19.TI.001>
- Cerfontaine, B., F. Collin 2018. "Cyclic and fatigue behaviour of rock materials: Review, interpretation and research perspectives". *Rock Mech Rock Eng* 51, 391–414. <https://doi.org/10.1007/s00603-017-1337-5>
- Jardine, R. J., A. Puech, Andersen, K. H 2012 "Cyclic loading of offshore piles: Potential effects and practical design". In *Offshore Site Investigation and Geotechnics*. Society of Underwater Technology, London, UK.
- Jardine, R. J., R. M. Buckley, S. Kontoe, P. Barbosa, F. C. Schroeder 2018. "Behaviour of piles driven in chalk". In *Engineering in Chalk: Proceedings of the Chalk Conference*, London, UK, pp. 33-51.
- Jardine, R. J., R. M. Buckley, T. Liu, T. Andolfsson, B. W. Byrne, S. Kontoe, R. A. McAdam, F. Schranz, K. Vinck 2023. "The axial behaviour of piles driven in chalk", *Géotechnique*. <https://doi.org/10.1680/jgeot.22.00041>
- Liu, T., R. Ahmadi-Naghadeh, K. Vinck, R. J. Jardine, S. Kontoe, R. M. Buckley, B. W. Byrne 2022a. "An experimental investigation into the behaviour of de-structured chalk under cyclic loading". Ahead of Print in *Géotechnique*. <https://doi.org/10.1680/jgeot.21.00199>
- Liu, T., R. J. Jardine, K. Vinck, S. K. Ackerley 2022b. "Optimization of advanced laboratory monotonic and cyclic triaxial testing on fine sands". *ASTM Geotechnical Testing Journal* 45(6). <https://doi.org/10.1520/GTJ20210190>
- Liu, T., P. M. V. Ferreira, K. Vinck, M. R. Coop, R. J. Jardine, S. Kontoe 2023a. "The behaviour of a low-to-medium density chalk under a wide range of pressure conditions". *Soils and Foundations*, 63(1). <https://doi.org/10.1016/j.sandf.2022.101268>
- Liu, T., R. J. Jardine, K. Vinck, R. Ahmadi-Naghadeh, S. Kontoe, R. M. Buckley, B. W. Byrne, R. A. McAdam 2023b. "Cyclic characterisation of low-to-medium density chalk for offshore driven pile design". *Offshore Site Investigation and Geotechnics Conference*, London, UK.
- Lord, J. A., C. R. L. Clayton, R. N. Mortimore 2002. "Engineering in chalk", CIRIA, C574.
- McAdam, R. A., R. M. Buckley, F. Schranz, B. W. Byrne, R. J. Jardine, S. Kontoe, T. Liu, K. Vinck, Crispin, J. 2022. "Monotonic and cyclic lateral loading of piles in low to medium density chalk", Final report to ALPACA and ALPACA Plus Sponsors, January 2022.
- Mortimore, R. N. 2012 "Making sense of chalk: a total-rock approach to its engineering geology". *Q. J. Engng Geol. Hydrogeol.* 45, No. 3, 252–334. <https://doi.org/10.1144/1470-9236/11-052>.
- Pedone, G., S. Kontoe, L. Zdravković, R. J. Jardine, K. Vinck, T. Liu. 2023 "Numerical modelling of laterally loaded piles driven in low-to-medium density fractured chalk". *Computers and Geotechnics*, 156, April 2023, 105252, <https://doi.org/10.1016/j.compgeo.2023.105252>.
- Vinck, K. 2021. "Advanced geotechnical characterisation to support driven pile design at chalk sites", PhD Thesis, Imperial College London.
- Vinck, K., T. Liu, R. J. Jardine, S. Kontoe, R. M. Buckley, B. W. Byrne, R. A. McAdam, P. Ferreira, M. Coop 2023. "The monotonic behaviour of a low- to medium-density chalk through in situ and laboratory characterisation". IS-Porto.